

## The dielectric function of AlSb from 1.4 to 5.8 eV determined by spectroscopic ellipsometry

Stefan Zollner, Chengtian Lin, Erich Schönherr, Alexandra Böhringer, and Manuel Cardona

Citation: *Journal of Applied Physics* **66**, 383 (1989); doi: 10.1063/1.343888

View online: <http://dx.doi.org/10.1063/1.343888>

View Table of Contents: <http://scitation.aip.org/content/aip/journal/jap/66/1?ver=pdfcov>

Published by the [AIP Publishing](#)

---

### Articles you may be interested in

Dielectric function in the spectral range (0.5–8.5)eV of an  $(\text{Al}_x\text{Ga}_{1-x})_2\text{O}_3$  thin film with continuous composition spread

*J. Appl. Phys.* **117**, 165307 (2015); 10.1063/1.4919088

Dielectric function of  $\text{LaAlO}_3$  from 0.8 to 6 eV between 77 and 700 K

*J. Vac. Sci. Technol. A* **30**, 061404 (2012); 10.1116/1.4754811

Dielectric response of AlSb from 0.7 to 5.0 eV determined by in situ ellipsometry

*Appl. Phys. Lett.* **94**, 231913 (2009); 10.1063/1.3153127

Optical dispersion relations for AlSb from  $E=0$  to 6.0 eV

*J. Appl. Phys.* **67**, 6427 (1990); 10.1063/1.345115

Optical constants for silicon at 300 and 10 K determined from 1.64 to 4.73 eV by ellipsometry

*J. Appl. Phys.* **53**, 3745 (1982); 10.1063/1.331113

---

The logo for AIP APL Photonics features the letters 'AIP' in a large, white, sans-serif font on the left. To its right is a vertical orange bar, followed by the words 'APL Photonics' in a smaller, white, sans-serif font. The background is a dark red with a bright yellow sunburst effect in the upper right corner.

*APL Photonics* is pleased to announce  
**Benjamin Eggleton** as its Editor-in-Chief



# The dielectric function of AlSb from 1.4 to 5.8 eV determined by spectroscopic ellipsometry

Stefan Zollner, Chengtian Lin, Erich Schönherr, Alexandra Böhringer, and Manuel Cardona

Max-Planck-Institut für Festkörperforschung, Heisenbergstrasse 1, D-7000 Stuttgart 80, Federal Republic of Germany

(Received 28 December 1988; accepted for publication 14 March 1989)

We have prepared AlSb substrates for optical measurements by chemomechanical polishing and etching. The quality of the surface was investigated with optical and electron microscopy and by Raman scattering and ellipsometry. We have measured the pseudodielectric function  $\langle \epsilon \rangle(\omega)$  of AlSb in the 1.4–5.8 eV photon-energy region with a spectroscopic ellipsometer. A peak value of  $\langle \epsilon_2 \rangle = 24.6$  at 4 eV was reached. We list the refractive index, the reflectivity, and the absorption coefficient, and obtain the critical point parameters at 300 K. Finally, we fit the index of refraction of AlSb at low photon energies with a semiempirical model.

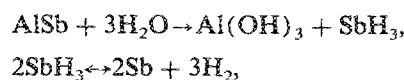
## I. INTRODUCTION

About five years ago, the dielectric functions  $\langle \epsilon \rangle(\omega)$  of Si, Ge, and most III-V semiconductors were measured in the 1.5–6 eV spectral range by Aspnes and Studna.<sup>1</sup> They showed that spectroscopic ellipsometry is a suitable tool for obtaining  $\langle \epsilon \rangle(\omega)$  with high accuracy. Such information is important for optical applications as well as of fundamental interest, since the band structure of a semiconductor is closely related to its optical properties.<sup>2</sup> Comparatively little work, however, has been done on the aluminum compounds.<sup>3–10</sup> The refractive index<sup>4</sup> and the absorption coefficient<sup>4,10</sup> of AlSb have been measured only below the direct gap (2.3 eV). For two reasons it has been difficult to obtain the optical constants in the visible and near UV region: (i) Large, high-quality single crystals are rare; (ii) the surfaces of these materials react rapidly with air, which makes it impossible to achieve abrupt bulk-air interfaces needed for precise reflection measurements. Therefore, Garriga *et al.*<sup>11</sup> have used a molecular beam epitaxy (MBE)-grown sample, consisting of a 1- $\mu\text{m}$ -thick AlAs layer covered by a protective 20-Å GaAs film, to measure the optical constants of AlAs.

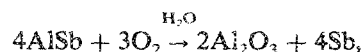
Many investigators of AlSb have measured surfaces cleaved in ultrahigh vacuum<sup>12</sup> or in an electrolyte,<sup>13</sup> as polished surfaces tend to tarnish in air. They have found, however, that pure samples are more corrosion resistant.<sup>14</sup> In this work we show that the usual wet-chemical etching procedure<sup>1</sup> yields AlSb (111) surfaces of sufficient quality for ellipsometric measurements. We discuss different processes of polishing and etching and give the results of our ellipsometric measurements at room temperature between 1.4 and 5.8 eV. We obtain the reflectivity, the absorption, and the complex index of refraction and perform a Kramers-Kronig<sup>15</sup> consistency check. From the numerically calculated second or third derivatives of  $\langle \epsilon \rangle(\omega)$ , we obtain the critical point (CP) parameters by performing a fit to analytical line shapes.<sup>16</sup> Finally, we fit the index of refraction at low photon energies with three models suggested recently for compound semiconductors.<sup>17–19</sup>

## II. POLISHING AND EXPERIMENTAL SETUP

AlSb slices with (111) faces were cut from a large, lightly ( $10^{16} \text{ cm}^{-3}$ ) In-doped single-crystal, which was grown by the Czochralski method as described elsewhere.<sup>20</sup> The samples were lapped with 3- $\mu\text{m}$  microgrit<sup>21</sup> on a glass plate. As AlSb is hygroscopic and reacts with humid air according to<sup>22</sup>



and with oxygen according to<sup>22</sup>



it is very difficult to polish. In the following, we discuss three different polishing methods. We emphasize that the quality of the surface obtained depends on the crystal quality. Polycrystalline samples, crystals with many dislocations, or small inclusions of metallic aluminum (about 10  $\mu\text{m}$  in diameter and visible with an electron microscope) are very hard to polish and/or do not withstand the etching procedures.

The simplest treatment for AlSb uses a commercial contact lens polish<sup>23</sup> and a black pad,<sup>24</sup> with minimum pressure and high speed, which will yield a shiny surface without scratches visible to the eye and an “orange peel” look, i.e., a wavy surface with little pits. Samples treated in this way are adequate to perform Raman scattering<sup>25,26</sup> or absorption experiments.<sup>10</sup> An alternative method uses a dish soap-based polish (95% dish detergent, 2% Repiglas,<sup>23</sup> 2% metal polish, and 1% water) under moderate pressure, yielding a shiny surface with a uniform pattern of scratches, only visible under the microscope, but without the “orange peel.”

The existence of overlayers on the surface is the crucial question in order to estimate the suitability of a sample for ellipsometric measurements. Therefore, the samples have to be etched *in situ* immediately before the measurement. Aspnes and Studna<sup>1</sup> have given prescriptions how to remove such oxide layers for a large number of semiconductors. As this procedure will enhance scratches on the surface, it is

desirable to have surfaces without microscopic scratches. (The ellipsometric results are not very much affected by scratches, but a sample with scratches will rapidly deteriorate when being etched.) Such scratchless surfaces could be obtained with the following method: After lapping, the samples were polished with 1- $\mu\text{m}$  diamond spray<sup>27</sup> on an RAM polishing disk<sup>28</sup> thoroughly soaked with water until the surface started to become bright, then with a solution of Repiglas<sup>23</sup> and NaOCl on a black pad.<sup>24</sup> The final treatment uses 90% Syton and 10% NaOCl, then 0.1% bromine in methanol (BrM) on a black pad. The microscopically smooth and scratchless surface was etched in a solution of 1 part of  $\text{HNO}_3$  (40%), 2 parts of HF (60%) in 2 parts of water for 2 min, then in 3 parts of  $\text{HNO}_3$  (40%) and 2 parts of HCl (40%) for about 1 min. Between the different steps the sample was rinsed with distilled water and blown dry. This procedure yielded a surface that was without pits or scratches under an optical microscope. The samples were also investigated with an electron microscope. The surface was smooth but a few small NaCl crystals (residue from the hypochlorite polishing) could be seen.

The chemical treatment immediately prior to the measurement is the same as the one suggested for InSb by Aspnes and Studna.<sup>29</sup> The sample was again polished for about 30 s with BrM on a black pad (BrMpad). The brown film forming on the surface could be removed by a short quench in ultrapure isopropanol. (The samples should not be immersed in isopropanol for more than a few minutes, as a shiny black film will form on the surface.) Then the sample was mounted on the sample holder in a windowless cell, the ellipsometer was calibrated,<sup>30</sup> and a wet chemical etching procedure as described in Ref. 31 was carried out while, simultaneously, ellipsometric data were taken. Following the "Biggest is Best" rule<sup>1</sup> we performed several etching steps until no significant increase of  $\langle\epsilon_2\rangle$  at the  $E_2$  peak (about 4 eV) was possible. Best results were obtained by etching with BrM, rinsing with isopropanol and blowing dry with a steady flow of pure dry nitrogen gas. We always started with

a more concentrated solution (about 0.1%) of BrM and later diluted this with more methanol. This probably indicated that in a higher concentration of BrM the stripping of polish residues, overlying oxide or hydroxide films, metallic or amorphous antimony, microscopic roughness, and damaged regions dominates, whereas a diluted BrM solution forms a passivating layer that protects the surface.<sup>31</sup> The surface stayed highly reflective for more than 1 h when nitrogen was continuously blown over the sample, but degraded within a few minutes in air. Macroscopic scratches and pits on the surface caused by the BrMpad treatment and the stripping procedure do not reduce the optical quality.

After etching, the system was calibrated again, since the optical properties of the surface had drastically changed during the etching process. Measurements were performed with an automatic spectroscopic ellipsometer of rotating-analyzer type<sup>1</sup> (RAE) in the 1.4–5.8 eV region. The setup and procedure have been described in detail elsewhere.<sup>32</sup> All the spectra were taken with a mesh of 5 or 10 meV at an angle of incidence of 67.5° and with the polarizer at 30° with respect to the plane of incidence.

### III. RESULTS AND DISCUSSION

The pseudodielectric function of AlSb, measured immediately after the etching process, is given in Fig. 1 (dotted lines) in the 1.4–5.8 eV photon-energy region. The two experimental spectra (measured with different gratings) do not match in the region of overlap because of different surface contamination. Our highest value of  $\langle\epsilon_2\rangle = 24.6$  at 4 eV indicates a very good surface quality. This peak value is comparable to that of GaSb (25.24 at 4.04 eV, see Ref. 1) and AlAs ( $\sim 30$  at 4.69 eV, see Ref. 11). The symbols at 4.0 and 4.2 eV give the highest results obtained during etching. We have therefore corrected<sup>33</sup> the already very good higher-energy experimental spectrum for a 0.3-nm-thick GaSb oxide overlayer. (The GaSb oxide data from Ref. 34 were used, as no information on the optical properties of native oxides on AlSb is available. In fact, the native oxides on all III-V compounds are very similar in this respect, at least at 4 eV and below.<sup>34,35</sup>) This corrected spectrum fits the experimental points at 4.0 and 4.2 eV very well. The lower-energy spectrum, taken at a different time, had to be corrected for 0.9-nm GaSb oxide in order to match the higher-energy one at 3.5 eV. The result is given by the solid line in Fig. 1. Although we cannot rule out that higher  $\epsilon_2$  peak values than 26 may be achieved by different preparation methods, we believe that improvements should be small. The corresponding reflectivity peak of  $R = 0.7$  at 4.33 eV is more than twice that of Ref. 12 and comparable to other zincblende materials.

The most exact previous measurements of the optical constants in the near-IR region below the indirect gap (1.6 eV) have been performed by Oswald and Schade.<sup>4</sup> Unfortunately, the data cannot be read with accuracy from the original figures. Therefore, we use their index of refraction as given in Ref. 7 and the absorption coefficients from Fig. 45 in Ref. 5. The index of refraction approaches  $n = 3.0$  below 10  $\mu\text{m}$  (see Refs. 4 and 5). Therefore,  $\epsilon(\infty) \sim 9$  seems to be the correct value of the IR dielectric constant. This is in good agreement with the independent result  $\epsilon(\infty) = 9.9$ , ob-

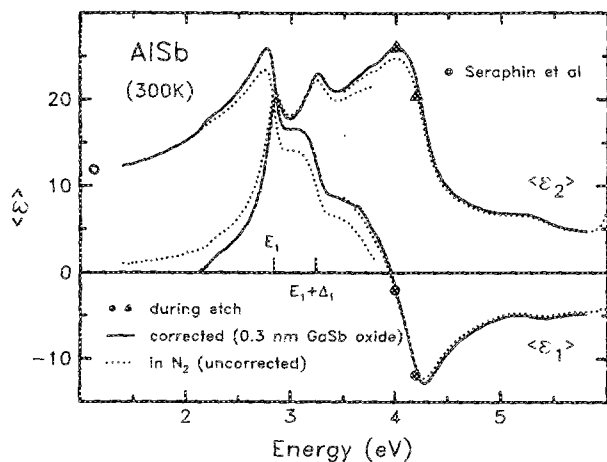


FIG. 1. Real and imaginary part of the pseudodielectric function of AlSb at 300 K as measured (dotted lines) and after a suitable correction (solid line) to reproduce the highest values obtained while etching ( $\bullet$ ,  $\blacktriangle$ ). The value of Ref. 7 at 1.13 eV is shown for comparison.

tained from an analysis<sup>8</sup> of the *reststrahlen* band around 30  $\mu\text{m}$ . That result<sup>8</sup> for the long-wavelength dielectric constant  $\epsilon(0) = 11.2$  also predicts the correct<sup>26</sup> Raman frequency for the zone-center longitudinal optical phonon via the Lyddane-Sachs-Teller relation.<sup>36</sup> The value of  $\epsilon(\infty) = 10.2$  from Refs. 6 and 9 is probably due to a misinterpretation of Oswald and Schade's original data. Indeed, Hass later<sup>37</sup> withdrew his own data<sup>9</sup> in favor of those of Ref. 8.

We have performed several checks on the consistency of our data. A Kramers-Kronig analysis<sup>15</sup> of  $\langle\epsilon_2\rangle$  gives a spectrum that is essentially displaced from the measured  $\langle\epsilon_1\rangle$  by a smooth background due to absorption above 5.6 eV, with the exception of the RAE artifact<sup>1</sup> below 2.5 eV and the region around 3.5 eV where the two spectra were matched.

TABLE I. Optical properties of AlSb, determined by ellipsometry, i.e., real and imaginary part of the pseudodielectric function  $\langle\epsilon\rangle$ , complex refractive index  $(n, k)$ , reflectivity  $R$ , and absorption coefficient  $\alpha$ . The absorption data below 1.7 eV were taken from Ref. 5, between 1.7 and 2.2 eV from Ref. 10.

$E$ (eV)	$\langle\epsilon_1\rangle$	$\langle\epsilon_2\rangle$	$n$	$k$	$R$	$\alpha$ ( $10^3 \text{ cm}^{-1}$ )
1.4	12.23	0.0007	3.50	0.0001	0.308	0.02
1.5	12.56	0.001	3.54	0.0002	0.312	0.03
1.6	12.91	0.002	3.60	0.0003	0.319	0.05
1.7	13.30	0.007	3.66	0.001	0.325	0.2
1.8	13.93	0.015	3.73	0.002	0.333	0.3
1.9	14.53	0.02	3.81	0.003	0.341	0.6
2.0	15.24	0.03	3.90	0.004	0.350	0.8
2.1	16.08	0.05	4.01	0.006	0.361	1.3
2.2	17.54	0.08	4.20	0.01	0.378	2.4
2.3	18.50	2.11	4.31	0.24	0.390	57.1
2.4	19.62	2.99	4.44	0.33	0.402	82.0
2.5	20.97	4.25	4.61	0.46	0.417	117.0
2.6	22.76	6.09	4.81	0.63	0.436	166.8
2.7	24.98	9.35	5.08	0.92	0.462	252.1
2.8	25.30	16.70	5.27	1.58	0.496	449.3
2.9	17.41	19.19	4.66	2.06	0.486	605.7
3.0	16.54	17.82	4.52	1.97	0.473	599.0
3.1	16.30	19.43	4.57	2.12	0.485	668.0
3.2	14.24	22.35	4.51	2.47	0.505	803.1
3.3	9.91	22.32	4.14	2.69	0.508	900.8
3.4	8.77	21.00	3.97	2.64	0.498	911.2
3.5	8.31	21.33	3.95	2.69	0.503	957.7
3.6	7.72	22.32	3.96	2.81	0.513	1028.7
3.7	6.63	23.35	3.91	2.97	0.525	1113.8
3.8	4.53	24.12	3.81	3.16	0.540	1218.3
3.9	2.16	25.22	3.71	3.40	0.560	1345.0
4.0	-1.56	26.00	3.50	3.71	0.588	1506.1
4.1	-6.14	25.24	3.15	4.00	0.621	1665.6
4.2	-11.16	21.99	2.60	4.22	0.662	1799.7
4.3	-12.73	15.94	1.96	4.07	0.691	1776.3
4.4	-11.20	11.81	1.59	3.70	0.688	1653.6
4.5	-9.41	9.81	1.45	3.39	0.669	1547.4
4.6	-8.11	8.71	1.38	3.16	0.648	1475.0
4.7	-7.17	7.97	1.33	2.99	0.629	1425.2
4.8	-6.40	7.42	1.30	2.84	0.611	1384.6
4.9	-5.76	7.06	1.29	2.72	0.592	1354.9
5.0	-5.29	6.85	1.30	2.64	0.576	1338.8
5.1	-5.00	6.77	1.31	2.59	0.565	1339.4
5.2	-4.95	6.74	1.31	2.58	0.563	1360.3
5.3	-5.15	6.53	1.26	2.59	0.574	1394.7
5.4	-5.30	6.02	1.17	2.58	0.589	1413.2
5.5	-5.18	5.51	1.09	2.52	0.593	1407.9
5.6	-5.00	5.12	1.04	2.46	0.594	1399.9
5.7	-4.84	4.88	1.01	2.42	0.592	1398.7
5.8	-4.81	4.78	1.00	2.40	0.593	1415.3

The rise of  $\langle\epsilon_2\rangle$  above 5.8 eV (see Fig. 1) is probably due to absorption in the quartz polarizer prisms. A Kramers-Kronig sum rule calculation<sup>15</sup> of the IR dielectric constant  $\epsilon_1(\infty)$  from our  $\langle\epsilon_2\rangle$  data gives a value of 9.2, which is in excellent agreement with experiments as discussed above. Using the same sum rule<sup>15</sup> to calculate the plasma frequency, however, we only obtain an effective valence electron density of 2.4 electrons per atom at 5.8 eV. This is similar to silicon<sup>38</sup> and due to having neglected absorption above 5.8 eV.

In Table I we give the corrected values of the pseudodielectric function as a function of energy, together with the complex index of refraction, the reflectivity, and the absorption coefficient calculated from  $\langle\epsilon\rangle$ . Due to the RAE artifact,<sup>1</sup> our values of  $\langle\epsilon_2\rangle$  are inaccurate below the direct gap and were replaced by data from other sources. Below 1.7 eV, we give the absorption coefficients from Ref. 5; between 1.7 and 2.2 eV, we use the values from Ref. 10.

In order to analyze the critical points (CPs) of AlSb, we have numerically calculated the second and third derivatives of the pseudodielectric function with respect to energy and performed a full line-shape fit, as described in detail in Ref. 39. The experimental data of  $d^2\epsilon_1/dE^2$  are shown in Fig. 2 (symbols). We have been able to resolve the  $E_0, E_1, E_1 + \Delta_1, E'_0, E'_0 + \Delta'_0, E_2$  and  $E'_1$  structures, whereas  $E_0 + \Delta_0$  is hidden under the  $E_1$  transition. Due to the RAE artifact<sup>1</sup> and to their weakness, the indirect transitions below the direct gap cannot be observed with our ellipsometer. The solid line gives the best fit to the data, the dashed line shows the imaginary part of the fitted line shape. The CP parameters obtained from the fit are given in Table II. They agree well with the values in the literature.<sup>40,41</sup> Just as for other semiconductors,<sup>42</sup> the CP energies are a little smaller than recent electroreflectance data,<sup>40</sup> but larger than older modulation spectroscopy results of Gavini and Cardona.<sup>43</sup>

#### IV. SEMIEMPIRICAL MODELS FOR THE REFRACTIVE INDEX

In the past years, a number of semiempirical models have been proposed to model the refractive index  $n$  of semi-

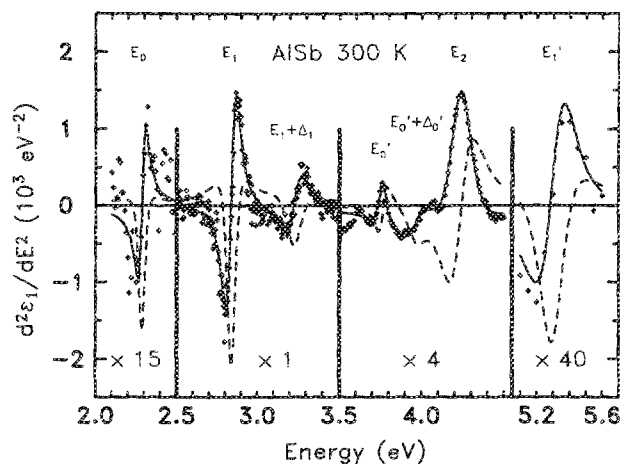


FIG. 2. Numerically calculated second derivative of  $\epsilon_1(\omega)$  of AlSb at 300 K (+). The  $E_0, E_1, E_1 + \Delta_1, E'_0, E'_0 + \Delta'_0, E_2$ , and  $E'_1$  critical points are indicated. The solid line gives the best fit to the data, the dashed line shows the imaginary part of the theoretical curve.

TABLE II. Interband critical point (CP) parameters of AlSb at 300 K, obtained from a fit of the numerically calculated third derivative of  $\langle \epsilon \rangle$  to analytical line shapes. The phase angle of  $E_1 + \Delta_1$  was forced to be equal to that of  $E_1$ . The amplitudes have the dimension  $\text{eV}^{-0.5}$  (1) for a 3D (2D) CP. The numbers in parentheses give the 95% confidence limits. See Ref. 40 for a comparison with other results.

CP	Energy (eV)	Broadening (meV)	Amplitude	Phase angle (deg)	Line shape
$E_0$	2.27(1)	30(10)	3(1)	30(20)	3D
$E_1$	2.838(2)	53(2)	6(1)	90(5)	2D
$E_1 + \Delta_1$	3.23(1)	88(8)	4(1)	90(5)	2D
$E'_0$	3.76(1)	34(5)	3(1)	120(20)	3D
$E'_0 + \Delta'_0$	3.97(3)	80(10)	9(3)	40(40)	3D
$E_2$	4.23(1)	120(10)	6(1)	170(5)	2D
$E'_1$	5.30(1)	150(10)	0.8(1)	108(7)	2D

conductors below the direct gap.<sup>17,18</sup> Such information is important for the design of laser or waveguide structures and optical experiments with AlSb. The model suggested by Adachi<sup>18</sup> is based on an approach used by Cardona<sup>15,44</sup> and explains the dispersion of  $n$  with the presence of the  $E_0$  and  $E_0 + \Delta_0$  critical points (CPs):

$$\epsilon_1(\omega) = A \{ f(\hbar\omega/E_0) + 0.5 [E_0/(E_0 + \Delta_0)]^{1.5} \times f[\hbar\omega/(E_0 + \Delta_0)] \} + B, \quad (1)$$

with

$$f(x) = \begin{cases} x^{-2} [2 - (1+x)^{1/2} - (1-x)^{1/2}], & \text{if } x < 1; \\ x^{-2} [2 - (1+x)^{1/2}], & \text{if } x > 1. \end{cases} \quad (2)$$

In these expressions,  $E_0 = 2.27$  eV is the energy of the direct gap (see Table II) and  $\Delta_0 = 0.65$  eV the spin-orbit splitting,<sup>45</sup> as determined from optical measurements. The factor of  $\frac{1}{2}$  is justified, because the mass of the split-off hole band is larger than the heavy-hole and smaller than the light-hole mass. A more accurate treatment<sup>15</sup> should allow this factor to vary between about 0.4 and 0.6, but this is complicated by the complex valence-band structure and the poor accuracy of the effective masses in AlSb.  $A$  is related to the transition matrix element and used as an adjustable parameter. A very rough estimate<sup>15</sup> with  $\mathbf{k}\cdot\mathbf{p}$  theory yields  $A = P^{-1} \simeq 2$ , where  $P$  is the momentum matrix element<sup>15</sup> (in atomic units) between the conduction band and any of the three valence bands.  $A$  could be effectively increased by excitonic interactions<sup>18</sup> or by the dispersion from higher-energy (e.g.,  $E_1$ ) transitions. The influence of the  $E_1$  transition should be stronger than for other semiconductors since this structure is very close to the  $E_0$  transition (see Table II).  $B$  is a constant background from higher-energy transitions. The parameters suggested by Adachi<sup>18</sup> describe the IR index of refraction,<sup>4</sup> but not the values measured by us. We have therefore adjusted the parameters  $A = 35.3$  and  $B = -1.1$  to the best overall fit (dotted line in Fig. 3). The agreement between model and experiment is very good well below the band gap, but close to the band gap the disagreement becomes intolerable. We thus conclude that  $A$  was chosen too large.

A different model<sup>17</sup> based on Van Vechten's dielectric theory<sup>46</sup> uses the expressions

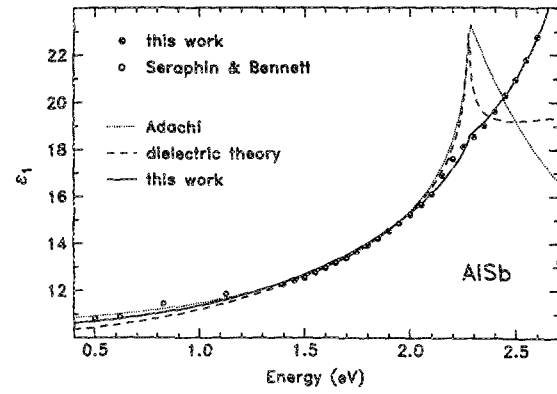


FIG. 3. Real part of the dielectric function of AlSb at 300 K from this work (●) and from Ref. 7 (○). Semiempirical models from Refs. 18 (dotted line) and 17 (dashed line) only fit the curve well below the band gap; a satisfactory model (solid line) has to take into account the  $E_1$  transitions.

$$\epsilon_1(\omega) = \epsilon_1(\infty) + \frac{\eta}{\pi} \left( (E_{\text{lim}}^2 - E_0^2) E^2 + \ln \left| \frac{E_{\text{lim}}^2 - E^2}{E_0^2 - E^2} \right| E^4 \right), \quad (3)$$

$$n_{\text{eff}} = \frac{D\pi}{\arctan[21 \text{ eV}(1.82/E_p)]}, \quad (4)$$

$$\frac{3E_p^2 n_{\text{eff}}}{8} = [\epsilon_1(\infty) - 1] \frac{E_{\text{lim}}^6 - E_0^6}{E_{\text{lim}}^4 - E_0^4},$$

$$\eta = 2\pi \frac{\epsilon_1(\infty) - 1}{E_{\text{lim}}^4 - E_0^4}. \quad (5)$$

Here  $\epsilon_1(\infty)$  is the IR dielectric constant,  $\eta$  the strength of the valence transitions, and  $E_{\text{lim}}$  the highest energy for interband transitions which can be obtained from the plasma frequency  $\hbar\omega_p = E_p = 13.82$  eV of the valence electrons<sup>15</sup> and an effective electron density  $n_{\text{eff}}$ . The IR dielectric constant  $\epsilon_1(\infty) = 9.9$  from Ref. 8 could not give a satisfactory fit to the data. We therefore used  $\epsilon_1(\infty) = 10.2$  from Ref. 6 although this is probably too large as discussed above. The factor  $D$ , taking into account the contribution of the  $d$  electrons to the valence electron density, can be calculated from the dielectric theory<sup>46</sup> ( $D = 1.19$ ), but in this work it was treated as an adjustable parameter. With  $D = 1.07$ , we obtain  $E_{\text{lim}} = 4.5$  eV. The quality of the fit thus obtained (dashed line in Fig. 3) is comparable to that of the interband CP model of Adachi.

As both of these models are inadequate, we add a second term to Eq. (1) for the influence of the  $E_1$  and  $E_1 + \Delta_1$  transitions. (In principle, two terms are necessary for these structures. In order to keep the model simple we choose an average gap.) The resulting contribution of the two-dimensional critical points  $E_1$  and  $E_1 + \Delta_1$  to  $\epsilon_1$  is<sup>19</sup>

$$\Delta\epsilon_1(\omega) = Cx_1^{-2} \ln \left( \frac{1 - (\hbar\omega/E_{\text{lim}})^2}{1 - x_1^2} \right),$$

with

$$x_1 = \frac{\hbar\omega}{E_1 + \Delta_1/2}. \quad (6)$$

The fit parameter  $C$  can again be estimated<sup>15</sup> with  $\mathbf{k}\cdot\mathbf{p}$  theory, with the result  $C\sim 6$ , which could be increased by excitonic enhancements of the  $E_1$  transitions.<sup>39</sup> In Eq. (6) we have introduced a cutoff energy  $E_{lim}$  which is justified as the parabolic bands of the  $E_1$  transition do not extend to infinity. We find  $E_{lim} = 4.6$  eV by imposing the constraint that the constant background  $B$  from higher-energy structures should be zero. The matrix element parameters obtained from the fit are  $A = 4.6$  and  $C = 15$ , somewhat larger than the  $\mathbf{k}\cdot\mathbf{p}$  estimates (as expected). Figure 3 shows that the agreement between this fit and the experiment is very good; the difference is actually smaller than the absolute accuracy of our measurement.

## V. CONCLUSION

We have developed a polishing method to obtain AlSb surfaces of high quality, which should be very useful for the preparation of surfaces for optical measurements as well as of substrates for epitaxial growth on AlSb. We have measured the pseudodielectric function of AlSb with a rotating-analyzer ellipsometer. The results are discussed and evaluated to give the critical point parameters of AlSb with high accuracy. The index of refraction below and near the direct gap can be described very well with a model that takes into account the dispersion of the  $E_0$ ,  $E_0 + \Delta_0$ , and  $E_1$  transitions.

## ACKNOWLEDGMENTS

We are grateful to W. Hönle, G. Sprater, and J. Quack for designing and constructing the windowless etching cell and to H. Hirt, P. Wurster, and M. Siemers for technical help. A. Keckes and E. Winckler performed the optical and electron microscopy work. One of us (S.Z.) would like to thank M. Garriga for many stimulating discussions and a critical reading of the manuscript.

<sup>1</sup>D. E. Aspnes and A. A. Studna, Phys. Rev. B **27**, 985 (1983).

<sup>2</sup>M. Cardona, *Modulation Spectroscopy* (Academic, New York, 1969).

<sup>3</sup>B. Monemar, Solid State Commun. **8**, 2121 (1970); R. E. Fern and A. Onton, J. Appl. Phys. **42**, 3499 (1971).

<sup>4</sup>F. Oswald and R. Schade, Z. Naturforsch. **9a**, 611 (1954).

<sup>5</sup>H. Welker and H. Weiss, in *Solid State Physics*, edited by F. Seitz and D. Turnbull (Academic, New York, 1956), Vol. 3, p. 1.

<sup>6</sup>T. S. Moss, *Optical Properties of Semi-Conductors* (Butterworths, London, 1961), p. 224.

<sup>7</sup>B. O. Seraphin and H. E. Bennett, in *Semiconductors and Semimetals*, edited by R. K. Willardson and A. C. Beer (Academic, New York, 1967), Vol. 3.

<sup>8</sup>W. J. Turner and W. E. Reese, Phys. Rev. **127**, 126 (1962).

<sup>9</sup>M. Hass and B. W. Hennis, J. Phys. Chem. Solids **23**, 1099 (1962).

<sup>10</sup>K. Strössner, S. Ves, C. K. Kim, and M. Cardona, Phys. Rev. B **33**, 4044 (1986).

<sup>11</sup>M. Garriga, P. Lautenschlager, M. Cardona, and K. Ploog, Solid State Commun. **61**, 157 (1987).

<sup>12</sup>T. E. Fischer, Phys. Rev. **139**, A1228 (1965).

<sup>13</sup>M. Cardona, F. H. Pollak, and K. L. Shaklee, Phys. Rev. Lett. **16**, 644 (1966).

<sup>14</sup>R. F. Blunt, H. P. R. Frederikse, J. H. Becker, and W. R. Hosler, Phys. Rev. **96**, 578 (1954).

<sup>15</sup>M. Cardona, in *Atomic Structure and Properties of Solids*, edited by E. Burstein (Academic, New York, 1972), p. 514.

<sup>16</sup>D. E. Aspnes, in *Handbook of Semiconductors*, edited by M. Balkanski (North-Holland, Amsterdam, 1980), Vol. 2, Chap 4A.

<sup>17</sup>D. Campi and C. Papuzza, J. Appl. Phys. **57**, 1305 (1985).

<sup>18</sup>S. Adachi, J. Appl. Phys. **53**, 5863 (1982); **58**, R1 (1985); **61**, 4869 (1987).

<sup>19</sup>K. Strössner, S. Ves, and M. Cardona, Phys. Rev. **32**, 6614 (1985). See also S. Adachi, Phys. Rev. B **35**, 7454 (1987).

<sup>20</sup>C. T. Lin, E. Schönherr, H. Bender, and C. Busch, J. Cryst. Growth **94**, 955 (1988).

<sup>21</sup>3  $\mu\text{m}$  Microgrit, Pieplow & Brandt, Henstedt-Ulzburg, FRG, dressed with ethylen glycol, some glycerine, and dish soap.

<sup>22</sup>*Gmelin Handbook of Inorganic Chemistry* (Chemie, Weinheim, 1936), Vol. 35A4, p. 632.

<sup>23</sup>Repiglas plastic contact lens polish, London and Scandinavian Metallurgic Co., London, UK.

<sup>24</sup>Polycon 100 polishing pad, Pieplow & Brandt, Henstedt-Ulzburg, FRG.

<sup>25</sup>V. I. Gavrilenko (private communication).

<sup>26</sup>S. Ves, K. Strössner, and M. Cardona, Solid State Commun. **57**, 483 (1986) and references therein.

<sup>27</sup>HYPREZ spray, diamond lapping compound, 1  $\mu\text{m}$ , ENGIS Ltd, Maidstone, Kent, UK.

<sup>28</sup>RAM polishing disk, Procédes et équipement pour les sciences et l'industries, POISAT-Grenoble, France.

<sup>29</sup>D. E. Aspnes and A. A. Studna, J. Vac. Sci. Technol. **20**, 488 (1982).

<sup>30</sup>D. E. Aspnes, J. Opt. Soc. Am. **64**, 812 (1974).

<sup>31</sup>D. E. Aspnes and A. A. Studna, Appl. Phys. Lett. **39**, 316 (1981).

<sup>32</sup>L. Viña, S. Logothetidis, and M. Cardona, Phys. Rev. B **30**, 1979 (1984).

<sup>33</sup>R. M. A. Azzam and N. M. Bazzara, *Ellipsometry and Polarized Light* (North-Holland, Amsterdam, 1977), p. 283.

<sup>34</sup>D. E. Aspnes, B. Schwartz, A. A. Studna, L. Derick, and L. A. Koszi, J. Appl. Phys. **48**, 3510 (1977).

<sup>35</sup>H. J. Lewerenz, D. E. Aspnes, B. Müller, D. L. Malm, and A. Helier, J. Am. Chem. Soc. **104**, 3325 (1982); H. J. Mattausch and D. E. Aspnes, Phys. Rev. B **23**, 1896 (1981).

<sup>36</sup>R. H. Lyddane, R. G. Sachs, and E. Teller, Phys. Rev. **59**, 673 (1941).

<sup>37</sup>M. Hass, in *Semiconductors and Semimetals*, edited by R. K. Willardson and A. C. Beer (Academic, New York, 1967), Vol. 3, p. 3.

<sup>38</sup>L. Viña and M. Cardona, Phys. Rev. B **29**, 6739 (1984).

<sup>39</sup>P. Lautenschlager, M. Garriga, S. Logothetidis, and M. Cardona, Phys. Rev. B **35**, 9174 (1987).

<sup>40</sup>A. Joulie, B. Girault, A. M. Joulie, and A. Zien-Eddine, Phys. Rev. B **25**, 7830 (1982).

<sup>41</sup>*Numerical Data and Functional Relationships in Science and Technology*, edited by O. Madelung (Springer, Berlin, 1986), Vol. 22a.

<sup>42</sup>S. Zollner, S. Gopalan, M. Garriga, J. Humlicek, and M. Cardona, in *19th International Conference on the Physics of Semiconductors*, Warsaw, edited by W. Zawadzki (Institute of Physics, Polish Academy of Sciences, Warsaw, 1988), Vol. 2, p. 1513, and references therein.

<sup>43</sup>A. Gavini and M. Cardona, Phys. Rev. B **1**, 672 (1970) and references therein.

<sup>44</sup>L. I. Korovin, Sov. Phys. Solid State **1**, 1202 (1960).

<sup>45</sup>K. C. Rustagi, P. Merie, D. Auvergne, and H. Mathieu, Solid State Commun. **18**, 1201 (1976).

<sup>46</sup>J. A. Van Vechten, Phys. Rev. **182**, 891 (1969).